ORGANIC CHEMISTRY

FRONTIERS







RESEARCH ARTICLE

View Article Online
View Journal | View Issue



Cite this: *Org. Chem. Front.*, 2019, **6**, 1266

Study of through-space substituent- π interactions using N-phenylimide molecular balances†

Jungwun Hwang, Ping Li, 🕩 * Erik C. Vik, Ishwor Karki and Ken D. Shimizu 🕩 *

Substituent $-\pi$ interactions associated with aromatic stacking interactions were experimentally measured using a small N-phenylimide molecular balance model system. The direct interaction of the substituent (NH₂, CH₃, OH, F, Br, CF₃ and NO₂) with an aromatic ring was measured in the absence of the aromatic stacking interactions in solution. The measured substituent $-\pi$ energies were found to correlate well with the Hammett $\sigma_{\rm m}$ parameter similar to the substituent effects observed in aromatic stacking systems. The persistent electrostatic trends in substituent effects can arise from the direct electrostatic interactions between substituents and opposing π -systems.

Received 3rd February 2019, Accepted 23rd March 2019 DOI: 10.1039/c9qo00195f

Introduction

rsc.li/frontiers-organic

Noncovalent interactions of aromatic surfaces play important roles in many areas in modern chemistry, biology, and materials science, 1-5 such as in the selectivity of chemical reactions,6 assembly and function of proteins,5,7-9 and construction of supramolecular architectures. 10,11 Therefore, studies of the nature of non-covalent aromatic interactions are important to more accurately design, model, and predict the behavior of supramolecular systems. 12-18 Aromatic stacking energies are heavily influenced by the presence of substituents on the interacting surfaces. 18-20 Experimental studies have observed that electron withdrawing substituents more strongly stabilize the stacking interaction in comparison to electron donating substituents which often manifested in a strong linear correlation between the measured interaction energy of substituted aromatic rings and the electrostatic Hammett substituent parameter $(\sigma_p \text{ or } \sigma_m)$. Seminal works by Hunter and Sanders have led to a qualitative model which theorized that the electrostatic substituent effects were due to the substituents polarizing the electrons in the attached aromatic ring (Fig. 1A, left). 27,28 Electron withdrawing groups increase the positive charge on the Sigma framework enhancing attraction to the opposing aromatic quadrupole and meanwhile decrease the negative charge on the π -cloud reducing repulsions between the opposing quadrupoles.

More recently, Wheeler and Houk developed a quantitative model which theorized that the substituent effects were due to the direct interactions of the substituents with the opposing

Department of Chemistry and Biochemistry, University of South Carolina, Columbia, SC 29208, USA. E-mail: shimizu@mail.chem.sc.edu, li246@mailbox.sc.edu † Electronic supplementary information (ESI) available. See DOI: 10.1039/c9q000195f

aromatic ring (Fig. 1A, right).²⁹ Computational studies have provided the strongest support for the Wheeler-Houk substitu-

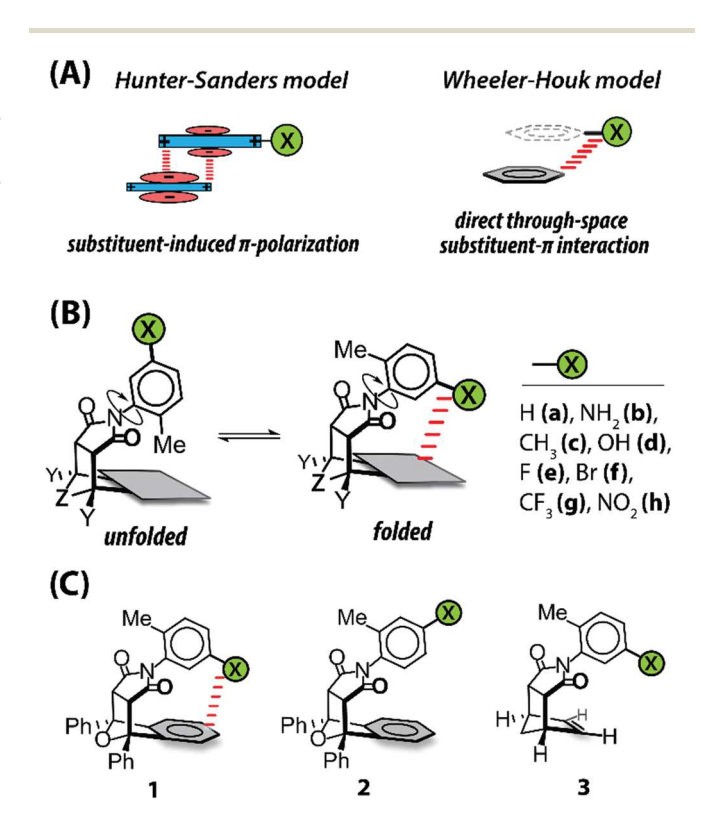


Fig. 1 (A) Schematic representations of two mechanistic hypotheses for aromatic substituent effects: Hunter–Sanders (left) and Wheeler–Houk models (right). (B) The folded–unfolded equilibrium of the N-phenylimide atropisomeric molecular balance model that can form and measure the intramolecular through-space substituent– π interactions in the folded state. (C) Structures of the folded substituent– π (1) and control balances (2 and 3).

ent effect model. In their initial report, Wheeler and Houk observed that the substituent effects were virtually identical in computational models where the substituent was attached to aromatic surface (broken line in Fig. 1B) or isolated without attaching to an aromatic ring. ²⁹ This demonstrated that the direct interaction of the substituents with the opposing aromatic surface could describe or explain the observed substituent effects.

Indirect approaches to experimentally testing the Wheeler-Houk model have been reported focusing on examining the consequences of the direct interaction model such as substituent effect distance dependence and additivity. ^{13,18,21}

However, direct methods of testing are challenging in experimental systems as they require measuring the substituent interactions without an attached aromatic surface. Nevertheless, the goal of this study was to attempt to design a model system that directly measures the interactions of substituents with π -surfaces (Fig. 1).

Results and discussion

Our bicyclic *N*-phenylimide molecular balance model system^{30–34} was chosen for the study of the substituent– π interactions (Fig. 1B). This versatile atropisomeric model system has found great success in the studies of various aromatic interactions including aromatic stacking,^{21,35} heterocycle– π ,³⁶

CH/D $-\pi$, 30,37,38 metal $-\pi$, 33 halogen $-\pi$, 39,40 chalcogen $-\pi$, 41 dispersion 42,43 and solvent effects. $^{44-47}$ Restricted rotation of the $C_{(phenyl)}$ – $N_{(imide)}$ single bond of the N-phenyl rotor leads to the formation of distinct unfolded and folded conformers. In the folded conformer, an intramolecular interaction forms between a substituent on the rotor and the aromatic shelf. In the unfolded conformer, the interacting groups are held apart by the rigid bicyclic framework. Therefore, the folded–unfolded equilibria provides a highly sensitive measure (± 0.02 kcal mol $^{-1}$) of the non-covalent interaction of interest in the folded conformer.

To measure the direct substituent– π interactions, substituents (X in Fig. 1B) with varying electronic properties were affixed to the 5-position of the *N*-phenyl rotor of balances **1b**–**g**. In the folded conformation, the substituent is positioned in proximity to the six-membered aromatic shelf, forming a through-space substituent– π interaction. Specifically, the balance system was designed to measure through-space interactions that do not involve direct van der Waals contacts. Verification of this design is provided *via* modelling shown in Fig. 4. In the unfolded conformation, the substituent is unable to reach the aromatic shelf.

In addition, two control balances (2 and 3) were designed to isolate the substituent– π interactions in balances **1a–h** from other factors that could influence the folded–unfolded equilibria (Fig. 2). Control balances **2a–h** contain the same series of substituents as balances **1a–h** but the substituents are fixed at

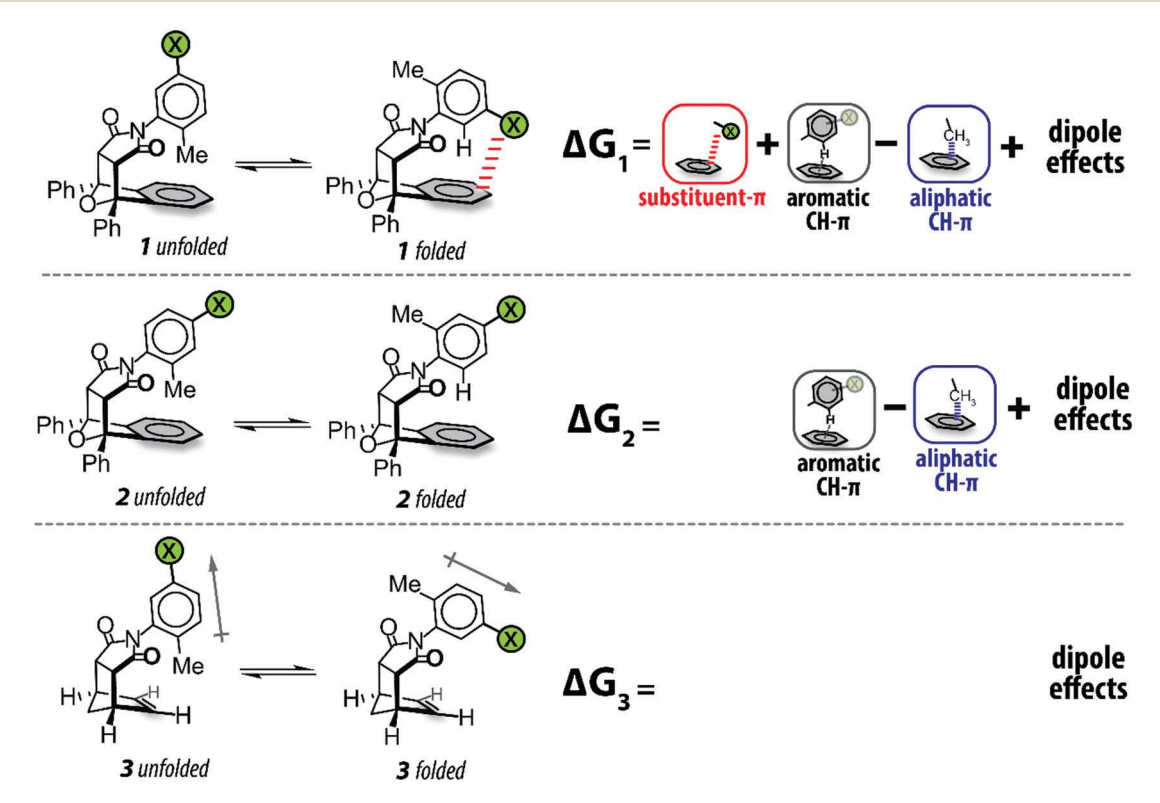


Fig. 2 Illustration of the experimental assessment of through-space substituent $-\pi$ interactions by comparing the folding energies (ΔG) between substituent $-\pi$ (1) and control balances (2 and 3). Note that the aliphatic CH $-\pi$ interaction occurred in the unfolded state and thus is denoted with a negative sign as it negatively contributed to the measured folding energy.

the 4-position of the N-phenyl rotor, which are further away from the aromatic shelf minimizing the intramolecular substituent- π interactions. The substituents in 2a-h are also on the rotational axis of the rotors eliminating their influence on the folded-unfolded equilibrium. Therefore, control balances 2a-h assist in isolating the through-bond polarization effects in balances 1a-h that modulate the intramolecular aliphatic and aromatic CH- π interactions of the rotors (Fig. 2).⁴⁶ Control balances 3a-h, on the other hand, have the substituents in the same position (5-position) as in balances 1a-h. However, balances 3a-h lack the six-membered aromatic shelf and thus cannot form intramolecular substituent- π interactions. Therefore, balances 3a-h assist in isolating the influences of the differences in molecular dipoles of folded and unfolded conformers in balances 1a-h.

Research Article

A key design feature in balances 1-3 was the 2-methyl groups on the N-phenyl rotors. These 'passive' methyl groups are reminiscent of the ortho-aryl methyl groups used in the design of Rebek's early molecular clefts to rigidify and preorganize their structures. 48,49 In balances 1-3, the 2-methyl groups are important to allow for accurate measurement of the folded/unfolded ratios by ¹H NMR. Specifically, the 2-methyl groups raise the rotational barrier of the rotors to ensure that the peaks for the folded and unfolded conformers are in slow exchange at room temperature. In addition, the folded and unfolded peaks for the 2-methyl protons are easily and accurately integrated as they are intense, baseline-separated singlets. One complication is that the 2-methyl groups do form intramolecular interactions with the aromatic shelves in the unfolded conformation. 30,32,33 However, the influence of noncovalent interactions of the 2-methyl groups can be measured separately using control balance 2 and isolated from the substituent- π interactions of interest.

Balances 1-3 were synthesized using previously described methods^{32,33} and fully characterized (see the ESI†). The folded/unfolded ratios for balances 1-3 were measured via integration of the ¹H NMR spectra in CDCl₃ at room temperature (25 °C). In balance 1, the 2-methyl group singlets for the folded and unfolded conformers were at 2.1 and 1.1 ppm, respectively.30-34 The unfolded peaks were assigned based on their upfield shift due to the shielding effects from the adjacent aromatic shelf in the unfolded conformer. Similar analyses were performed to measure the folding ratios of balances 2 and 3. The corresponding folding energies were calculated $(\Delta G = -RT \ln[folded/unfolded])$ and are listed in Table 1. Note that unsubstituted balances 1a and 2a are the same molecule and thus have the same folding energies.

The variations in the folding energies for balances 1a-h (X = H, NH₂, CH₃, OH, F, Br, CF₃, and NO₂) provided the first evidence that balance 1 could measure the direct substituent- π interactions. All of the substituted balances 1b-h were more folded with lower folding energies than the unsubstituted balance 1a. In addition, balances 1g and 1h with strongest electron-withdrawing substituents, CF₃ and NO_2 , showed the largest stabilizations ($\Delta\Delta G = -0.22$ and -0.24 kcal mol⁻¹) of the folded conformation. Similar to the

Table 1 1 H NMR measured folding energies for the substituent $-\pi$ balances **1** (ΔG_1 , kcal mol⁻¹) and control balances **2** (ΔG_2 , kcal mol⁻¹) and **3** $(\Delta G_3$, kcal mol⁻¹) at 25 °C in CDCl₃. Error for measured folding energies was within ± 0.02 kcal mol⁻¹

Substituent (X)		ΔG_1	ΔG_2	ΔG_3
(a)	Н	-0.84	-0.84	-0.02
(b)	NH_2	-0.85	-0.80	-0.04
(c)	CH_3^2	-0.89	-0.83	-0.05
(d)	OH	-0.90	-0.82	-0.05
(e)	F	-0.97	-0.84	-0.05
(f)	Br	-0.95	-0.83	-0.06
(g)	CF_3	-1.06	-0.84	0.02
(h)	NO_2	-1.08	-0.81	-0.03
` /	_			

substituent effect trends observed in aromatic stacking interactions, $^{13,18,19,21-23,50}$ the Hammett plot with $\sigma_{\rm m}$ was linear with a negative slope as the electron-withdrawing substituents stabilized the intramolecular substituent- π interactions (Fig. 3, red circles).

To examine the possibility that the variations in folding energies for balances 1a-h were due to other interactions, the folding energies of the control balances 2a-h and 3a-h were measured. In the case of control balances 2a-h, the substituents are further from the aromatic shelf minimizing their influence on the folding equilibrium. However, the substituents are still attached to the rotor and could polarize C-H

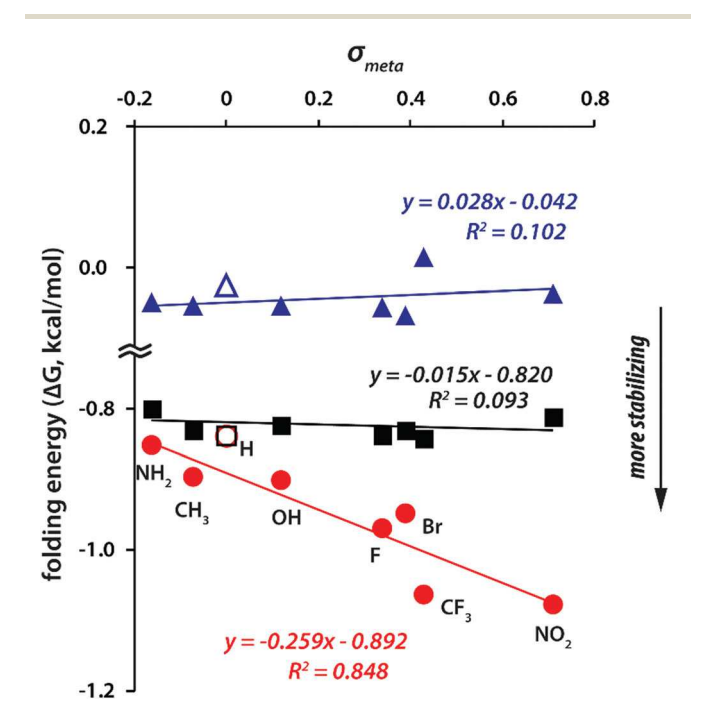


Fig. 3 Hammett plots of the measured folding energies (ΔG) of balance 1 and control balances 2 and 3 with the electrostatic $\sigma_{\rm m}$ parameter: substituted balances 1b-h (red filled circles), unsubstituted balance 1a (red open circle), substituted 2b-h (black filled squares). unsubstituted 2a (black open square), substituted 3b-h (blue solid triangles), unsubstituted 3a (blue open triangle). The unsubstituted balances 1a, 2a, and 3a were excluded from the linear regression.

bonds that form the intramolecular aromatic and aliphatic CH-π interactions. 32,47 The folding energies for 2a-h did not vary considerably with differing substituents, and the Hammett plot for 2a-h was flat (Fig. 3, black squares). This demonstrated that the influence of substituents on the $CH-\pi$ interactions of the rotor were either negligible or cancelled each other out.

The possibility that the substituent effects in balances 1a-h were due to the differences in dipole between the folded and unfolded conformers was examined using control balances 3a-h. These control balances contain the same substituents at the same 5-position as balances 1a-h and hence should have similar differences in dipole as balances 1a-h. However, control balances 3a-h do not contain an aromatic shelf and thus cannot form intramolecular substituent- π interactions. The measured folding energies for 3a-h (ΔG_3) showed very little variation (-0.05 to 0.02 kcal mol⁻¹), indicating that differences in dipole of the two conformers had very little influence on the folding equilibrium. The Hammett plot for 3a-h was more scattered but still flat (Fig. 3, blue triangles). Similar substituent trends were observed for all three balances 1, 2, and 3 in different solvent systems (Fig. S1 in ESI†).

Lastly, the possibility that the substituent trends in 1a-h were due to the dispersion or solvophobic interactions between the substituent and the aromatic shelf was examined. In contrast to the Hammett plots with $\sigma_{\rm m}$, the folding energies of balances 1a-h showed little correlation to the substituent molecular refractivity (MR),51 a parameter commonly correlated with the size and therefore to the dispersion and solvophobic interactions of the substituent. The correlation plot with MR showed a very poor linear correlation ($R^2 = 0.030$, Fig. 4A). Furthermore, the molecular modeling studies (Fig. 4B) demonstrated that the substituents did not make direct contact with the aromatic shelves. The geometries of the folded conformers of the 5-substituted balances 1b-h were optimized at BL3YP/6-31G* level of theory and confirmed by frequency analysis. In all cases, the 5-substituent of the N-phenyl rotor was rigidly held in close proximity of the shelf arene but did not form any direct van der Waals contacts. The closest atom-to-atom distance between the substituents and the aromatic shelves ranged from 3.63 to 5.03 Å in the folded conformers. The modelling results helped explain the minimal dispersion or solvophobic effects as these interactions have been found to be very weak when the interacting surfaces are not in van der Waals contacts. 13,42,52-55

The above assessments suggest that the substituent effects in balances 1a-h were due to the direct electrostatic interactions of the substituents with the aromatic shelves. These substituent- π interactions appear to be similar to those observed in stacking interactions. Therefore, the magnitude of the electrostatic substituent- π interactions in balances 1a-h were compared with our previously measured substituent effects in aromatic stacking interactions. 21,43 Specifically, the slope of the Hammett plots for balances 1b-g were compared with those for the substituent effects for stacking interactions measured previously within the same in the N-phenyl imide balances model systems under similar conditions.²¹ The slope

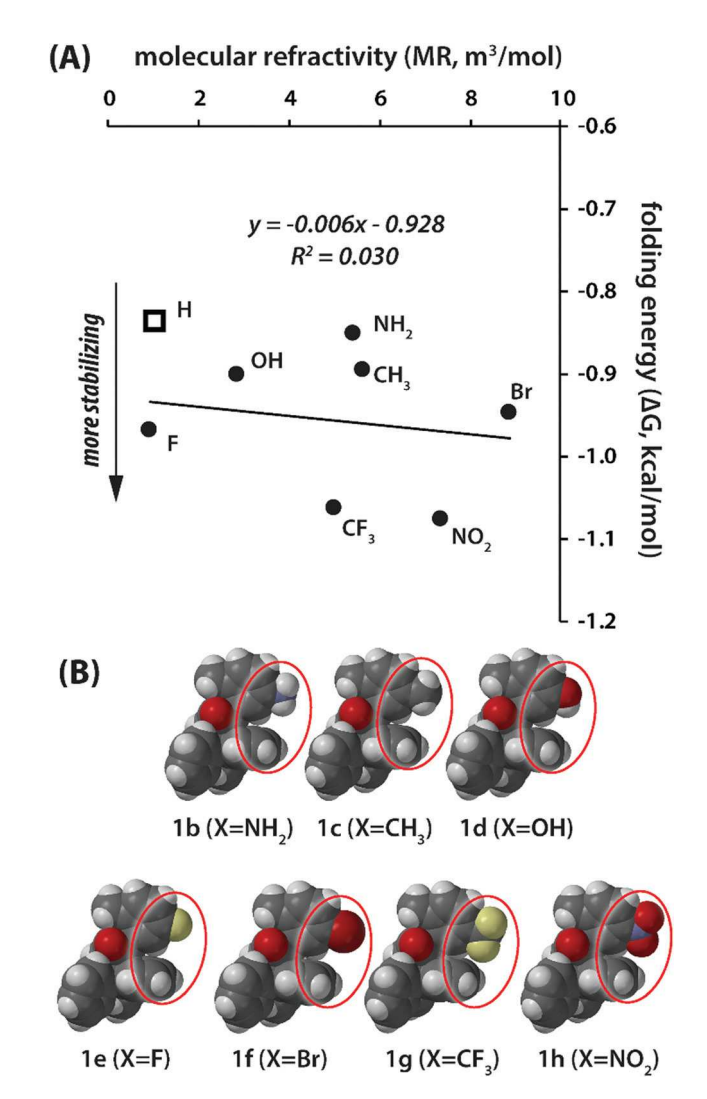


Fig. 4 (A) Correlation plots of folding energies (ΔG) of substituent- π balances 1b-h with the dispersion/polarizability molecular refractivity (MR) parameter. (B) Optimized structures (BL3YP/6-31G*) of folded substituent $-\pi$ balances **1b-h** (in spacefill model) highlighting the absence of direct van der Waals contact between the substituent and π -shelf.

for balances 1a-h was -0.259 kcal mol⁻¹, which was were significantly smaller than the slopes for the aromatic stacking interactions (slopes: -0.948 and -0.551 kcal mol⁻¹ for metaand para-substituents).21 These differences appear to be related to the distance of the substituents from the opposing π -system. The closest atom-to-atom distance for the methyl substituent was 3.71 Å in 1c, 3.36 Å in the para-methyl stacking balance, and 2.56 Å in the meta-methyl stacking balance according to X-ray crystal structures. 32,43 Thus, the weaker substituent-π interactions in balances 1a-h can be easily comprehended when the larger interaction distances were taken

Due to the experimental constraints of the framework, the substituent-π interaction geometry and distance were not identical to those in the computational studies by Wheeler and

Houk²⁹ and others. 56,57 Despite these differences, the observations of electrostatic substituent trends in the molecular balances still provide support for the Wheeler-Houk direct substituent- π interaction model. The electrostatic nature of these through-space interactions are still present and relevant at longer distances and varying geometries. Interestingly, Wheeler and Houk's initial report on the direct substituent- π hypothesis was based on a non-equilibrium geometry in which the aromatic rings were directly stacked on top of each other. The aligned stacking dimer allows for one of the closest substituent- π distances and thus maximum interaction energy. Wheeler has since tested that through-space electrostatic interactions at varying geometries and distances, 58,59 and found that the through-space electrostatic interactions dominate as long as the substituents do not form close contacts or engage intense exchange and dispersion interactions⁶⁰ with the opposing surfaces. However, as mentioned earlier, the distance dependence of substituent- π interactions is evident when comparing the electrostatic substituent trends in balances 1a-h and previously reported aromatic stacking balances²¹ that have much shorter interaction distances.

Conclusions

Research Article

In summary, a series of N-phenylimide molecular balances were developed to experimentally measure the substituent- π through-space interactions in solution. Possible interferences from through-bond electrostatic modulation of CH-π interactions and molecular dipoles were ruled out using control balances. The direct substituent- π interactions were weakly stabilizing (up to -0.27 kcal mol⁻¹ in CDCl₃). The substituent effects correlate well with the electrostatic substituent parameter $\sigma_{\rm m}$ and poorly with the dispersion/polarizability parameter MR. The electrostatic character of the substituent- π interactions were consistent with the theoretical prediction of direct substituent- π interactions. Further studies are currently underway to examine direct substituent- π interactions at shorter distances and in aqueous environments to quantify the dispersion and solvophobic contributions.

Conflicts of interest

There are no conflicts to declare.

Acknowledgements

The authors acknowledge the support of the National Science Foundation grants CHE 1709086 and CHE 1310139.

References

1 E. A. Meyer, R. K. Castellano and F. Diederich, Angew. Chem., Int. Ed., 2003, 42, 1210-1250.

- 2 L. M. Salonen, M. Ellermann and F. Diederich, Angew. Chem., Int. Ed., 2011, 50, 4808-4842.
- 3 B. L. Schottel, H. T. Chifotides and K. R. Dunbar, Chem. Soc. Rev., 2008, 37, 68-83.
- 4 A. S. Mahadevi and G. N. Sastry, Chem. Rev., 2013, 113, 2100-2138.
- 5 T. J. Mooibroek, P. Gamez and J. Reedijk, CrystEngComm, 2008, 10, 1501-1515.
- 6 A. J. Neel, M. J. Hilton, M. S. Sigman and F. D. Toste, Nature, 2017, 543, 637-646.
- 7 S. K. Burley and G. A. Petsko, Science, 1985, 229, 23-28.
- 8 M. Nishio, Y. Umezawa, J. Fantini, M. S. Weiss and P. Chakrabarti, Phys. Chem. Chem. Phys., 2014, 16, 12648-
- 9 J. P. Gallivan and D. A. Dougherty, Proc. Natl. Acad. Sci. U. S. A., 1999, 96, 9459-9464.
- 10 Z. Chen, A. Lohr, C. R. Saha-Moller and F. Würthner, Chem. Soc. Rev., 2009, 38, 564-584.
- 11 M. Xue, Y. Yang, X. D. Chi, Z. B. Zhang and F. H. Huang, Acc. Chem. Res., 2012, 45, 1294-1308.
- 12 C. D. Sherrill, Acc. Chem. Res., 2013, 46, 1020-1028.
- 13 J. Hwang, P. Li and K. D. Shimizu, Org. Biomol. Chem., 2017, 15, 1554-1564.
- 14 H.-J. Schneider, Acc. Chem. Res., 2013, 46, 1010-1019.
- 15 F. Biedermann and H.-J. Schneider, Chem. Rev., 2016, 116, 5216-5300.
- 16 M. L. Waters, Curr. Opin. Chem. Biol., 2002, 6, 736-741.
- 17 S. Ehrlich, J. Moellmann and S. Grimme, Acc. Chem. Res., 2013, 46, 916-926.
- 18 K. D. Shimizu, P. Li and J. Hwang, in *Aromatic Interactions:* Frontiers in Knowledge and Application, ed. D. W. Johnson and F. Hof, The Royal Society of Chemistry, Cambridge, 2017, pp. 124-171.
- 19 S. L. Cockroft, J. Perkins, C. Zonta, H. Adams, S. E. Spey, C. M. R. Low, J. G. Vinter, K. R. Lawson, C. J. Urch and C. A. Hunter, Org. Biomol. Chem., 2007, 5, 1062-1080.
- 20 S. E. Wheeler, Acc. Chem. Res., 2013, 46, 1029-1038.
- 21 J. Hwang, P. Li, W. R. Carroll, M. D. Smith, P. J. Pellechia and K. D. Shimizu, J. Am. Chem. Soc., 2014, 136, 14060-14067.
- 22 L. J. Riwar, N. Trapp, B. Kuhn and F. Diederich, Angew. Chem., Int. Ed., 2017, 56, 11252-11257.
- 23 S. L. Cockroft, C. A. Hunter, K. R. Lawson, J. Perkins and C. J. Urch, J. Am. Chem. Soc., 2005, 127, 8594-8595.
- 24 F. Cozzi, M. Cinquini, R. Annunziata, T. Dwyer and J. S. Siegel, J. Am. Chem. Soc., 1992, 114, 5729-5733.
- 25 F. Cozzi, M. Cinquini, R. Annuziata and J. S. Siegel, J. Am. Chem. Soc., 1993, 115, 5330-5331.
- 26 B. W. Gung, X. Xue and H. J. Reich, J. Org. Chem., 2005, 70, 3641-3644.
- 27 C. A. Hunter and J. K. M. Sanders, J. Am. Chem. Soc., 1990, 112, 5525-5534.
- 28 C. A. Hunter, K. R. Lawson, J. Perkins and C. J. Urch, J. Chem. Soc., Perkin Trans. 2, 2001, 5, 651-669.
- 29 S. E. Wheeler and K. N. Houk, J. Am. Chem. Soc., 2008, 130, 10854-10855.

- 30 C. Zhao, R. M. Parrish, M. D. Smith, P. J. Pellechia, C. D. Sherrill and K. D. Shimizu, *J. Am. Chem. Soc.*, 2012, 134, 14306–14309.
- 31 C. Zhao, P. Li, M. D. Smith, P. J. Pellechia and K. D. Shimizu, *Org. Lett.*, 2014, **16**, 3520–3523.
- 32 P. Li, J. Hwang, J. M. Maier, C. Zhao, D. V. Kaborda, M. D. Smith, P. J. Pellechia and K. D. Shimizu, *Cryst. Growth Des.*, 2015, **15**, 3561–3564.
- 33 J. M. Maier, P. Li, J. Hwang, M. D. Smith and K. D. Shimizu, J. Am. Chem. Soc., 2015, 137, 8014–8017.
- 34 J. M. Maier, P. Li, J. S. Ritchey, C. J. Yehl and K. D. Shimizu, *Chem. Commun.*, 2018, 54, 8502–8505.
- 35 W. R. Carroll, P. Pellechia and K. D. Shimizu, *Org. Lett.*, 2008, **10**, 3547–3550.
- 36 P. Li, C. Zhao, M. D. Smith and K. D. Shimizu, *J. Org. Chem.*, 2013, **78**, 5303–5313.
- 37 P. Li, T. M. Parker, J. Hwang, F. Deng, M. D. Smith, P. J. Pellechia, C. D. Sherrill and K. D. Shimizu, *Org. Lett.*, 2014, 16, 5064–5067.
- 38 W. R. Carroll, C. Zhao, M. D. Smith, P. J. Pellechia and K. D. Shimizu, *Org. Lett.*, 2011, 13, 4320–4323.
- 39 P. Li, J. M. Maier, E. C. Vik, C. J. Yehl, B. E. Dial, A. E. Rickher, M. D. Smith, P. J. Pellechia and K. D. Shimizu, *Angew. Chem., Int. Ed.*, 2017, 56, 7209–7212.
- 40 H. Sun, A. Horatscheck, V. Martos, M. Bartetzko, U. Uhrig, D. Lentz, P. Schmieder and M. Nazare, *Angew. Chem., Int. Ed.*, 2017, 56, 6454–6458.
- 41 J. Hwang, P. Li, M. D. Smith, C. E. Warden, D. A. Sirianni, E. C. Vik, J. M. Maier, C. J. Yehl, C. D. Sherrill and K. D. Shimizu, J. Am. Chem. Soc., 2018, 140, 13301–13307.
- 42 J. Hwang, B. E. Dial, P. Li, M. E. Kozik, M. D. Smith and K. D. Shimizu, *Chem. Sci.*, 2015, **6**, 4358–4364.
- 43 J. Hwang, P. Li, M. D. Smith and K. D. Shimizu, *Angew. Chem.*, *Int. Ed.*, 2016, 55, 8086–8089.

- 44 J. M. Maier, P. Li, E. C. Vik, C. J. Yehl, S. M. S. Strickland and K. D. Shimizu, *J. Am. Chem. Soc.*, 2017, 139, 6550– 6553.
- 45 B. U. Emenike, S. N. Bey, B. C. Bigelow and S. V. S. Chakravartula, *Chem. Sci.*, 2016, 7, 1401–1407.
- 46 B. U. Emenike, S. N. Bey, R. A. Spinelle, J. T. Jones, B. Yoo and M. Zeller, *Phys. Chem. Chem. Phys.*, 2016, 18, 30940–30945.
- 47 B. U. Emenike, R. A. Spinelle, A. Rosario, D. W. Shinn and B. Yoo, J. Phys. Chem. A, 2018, 122, 909–915.
- 48 J. Rebek, Science, 1987, 235, 1478-1484.
- 49 J. Rebek, in *Inclusion Phenomena and Molecular Recognition*, ed. J. L. Atwood, Springer US, Boston, MA, 1990, pp. 1–15.
- 50 M. Harder, M. A. C. Corrales, N. Trapp, B. Kuhn and F. Diederich, *Chem. Eur. J.*, 2015, **21**, 8455–8463.
- 51 M. Charton and B. I. Charton, *J. Org. Chem.*, 1979, 44, 2284–2288.
- 52 L. Yang, C. Adam, G. S. Nichol and S. L. Cockroft, *Nat. Chem.*, 2013, 5, 1006–1010.
- 53 L. Yang, C. Adam and S. L. Cockroft, *J. Am. Chem. Soc.*, 2015, 137, 10084–10087.
- 54 L. Yang, J. B. Brazier, T. A. Hubbard, D. M. Rogers and S. L. Cockroft, *Angew. Chem., Int. Ed.*, 2016, 55, 912–916.
- 55 R. Pollice, M. Bot, I. J. Kobylianskii, I. Shenderovich and P. Chen, J. Am. Chem. Soc., 2017, 139, 13126–13140.
- 56 M. O. Sinnokrot and C. D. Sherrill, J. Am. Chem. Soc., 2004, 126, 7690–7697.
- 57 M. Watt, L. K. Hardebeck, C. C. Kirkpatrick and M. Lewis, J. Am. Chem. Soc., 2011, 133, 3854–3862.
- 58 S. E. Wheeler, J. Am. Chem. Soc., 2011, 133, 10262-10274.
- 59 S. E. Wheeler and J. W. G. Bloom, J. Phys. Chem. A, 2014, 118, 6133-6147.
- 60 S. A. Arnstein and C. D. Sherrill, *Phys. Chem. Chem. Phys.*, 2008, 10, 2646–2655.